Utilizing Furfural-based Bifuran Diester as Monomer and Comonomer for High-Performance Bioplastics: Properties of Poly(butylene furanoate), Poly(butylene bifuranoate), and their Copolyesters

Tuomo P. Kainulainen,[a] Terttu I. Hukka,[b] Hüsamettin D. Özeren,[c] Juho A. Sirviö,[d] Mikael S. Hedenqvist,[c] Juha P. Heiskanen*,[a]

[a]Research Unit of Sustainable Chemistry, University of Oulu, P.O. Box 4300, FI-90014 Oulu, Finland

[b]Laboratory of Chemistry and Bioengineering, Tampere University of Technology, P.O. Box 541, FI-33101 Tampere, Finland

[c]Department of Fibre and Polymer Technology, School of Engineering Sciences in Chemistry, Biotechnology and Health, KTH Royal Institute of Technology, SE-100 44 Stockholm, Sweden

[d]Fibre and Particle Engineering Research Unit, University of Oulu, P.O. Box 4300, FI-90014 Oulu, Finland

Table of Contents

Figure S1. ^{1}H NMR spectrum of dimethyl 2,5-furandicarboxylate, $CDCl_3$:

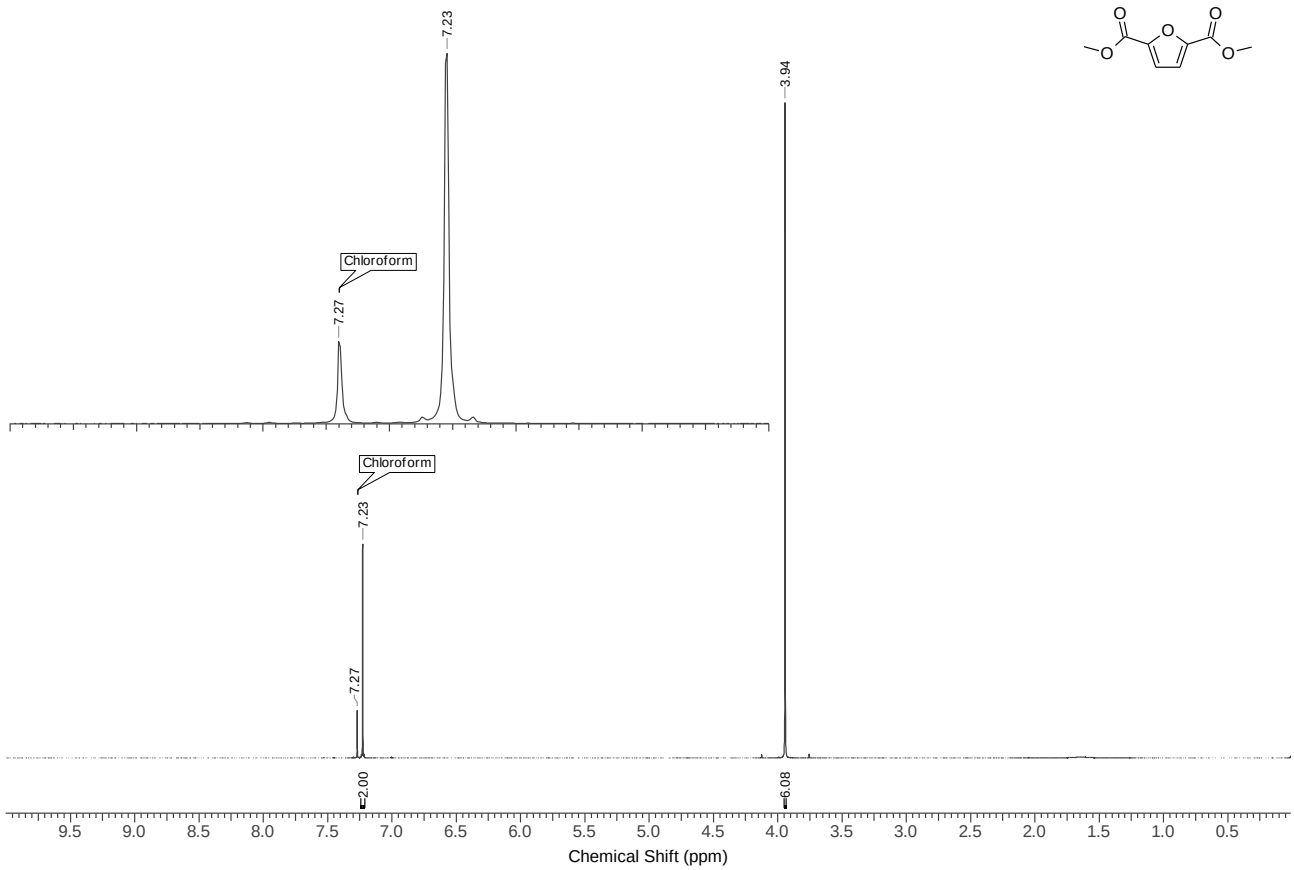

Figure S2. ^{1}H NMR spectrum of dimethyl 2,2'-bifuran-5,5'-dicarboxylate, $CDCl_3$:

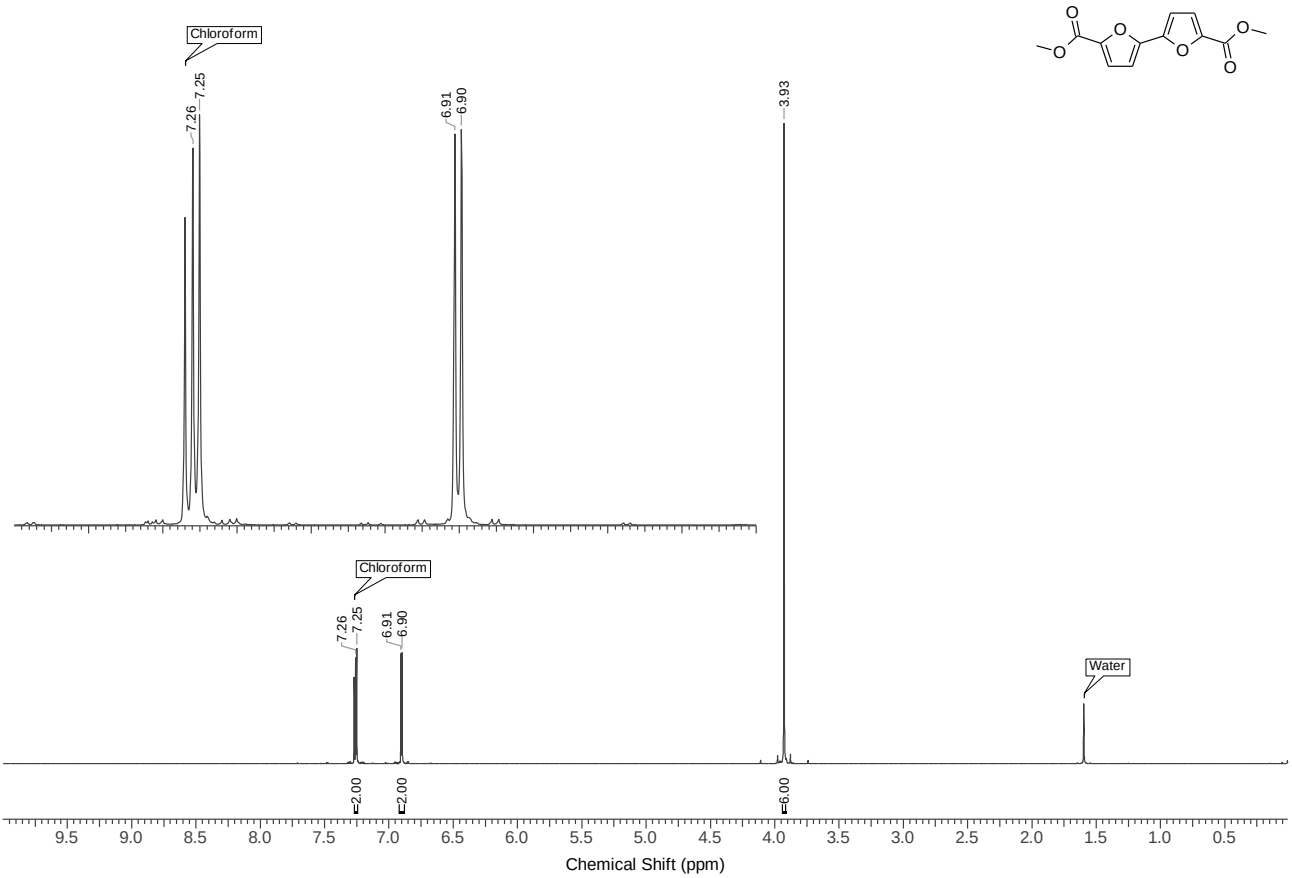

Figure S3a. Poly(butylene furanoate) (PBF) ^{1}H NMR spectrum, CF_3COOD:

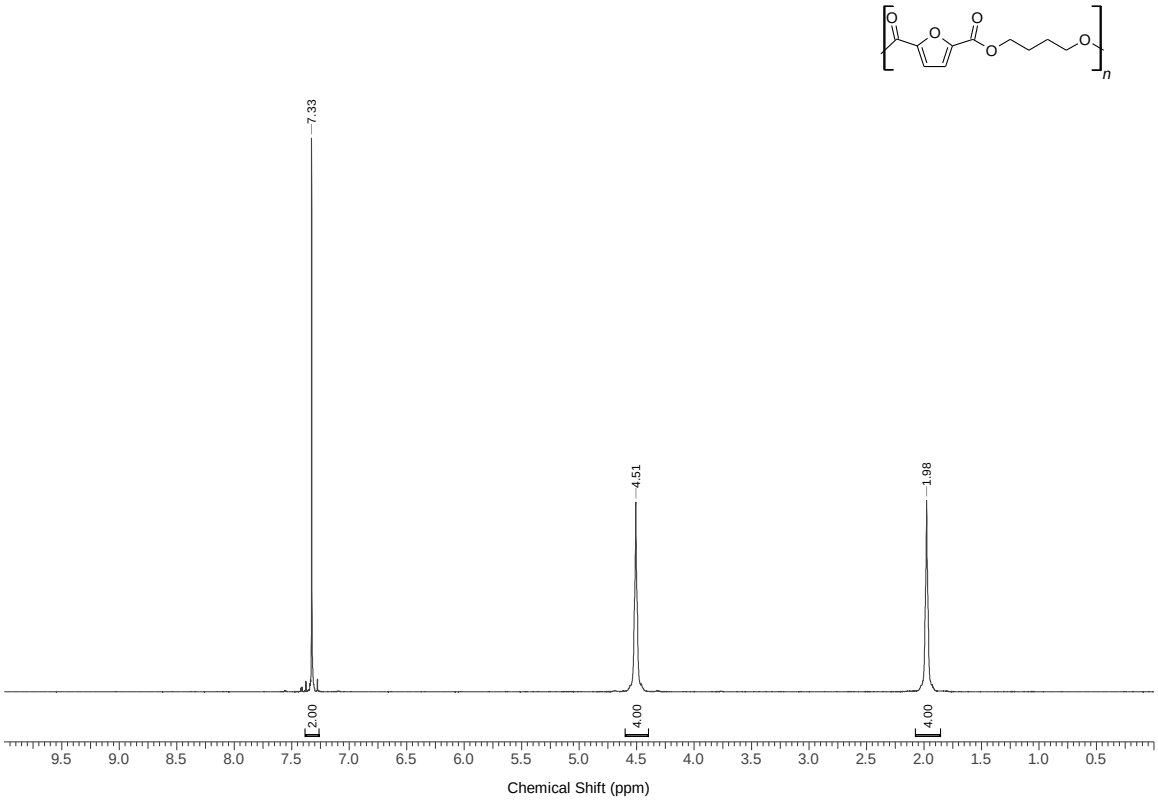

Figure S3b. Poly(butylene furanoate) (PBF) FTIR spectrum:

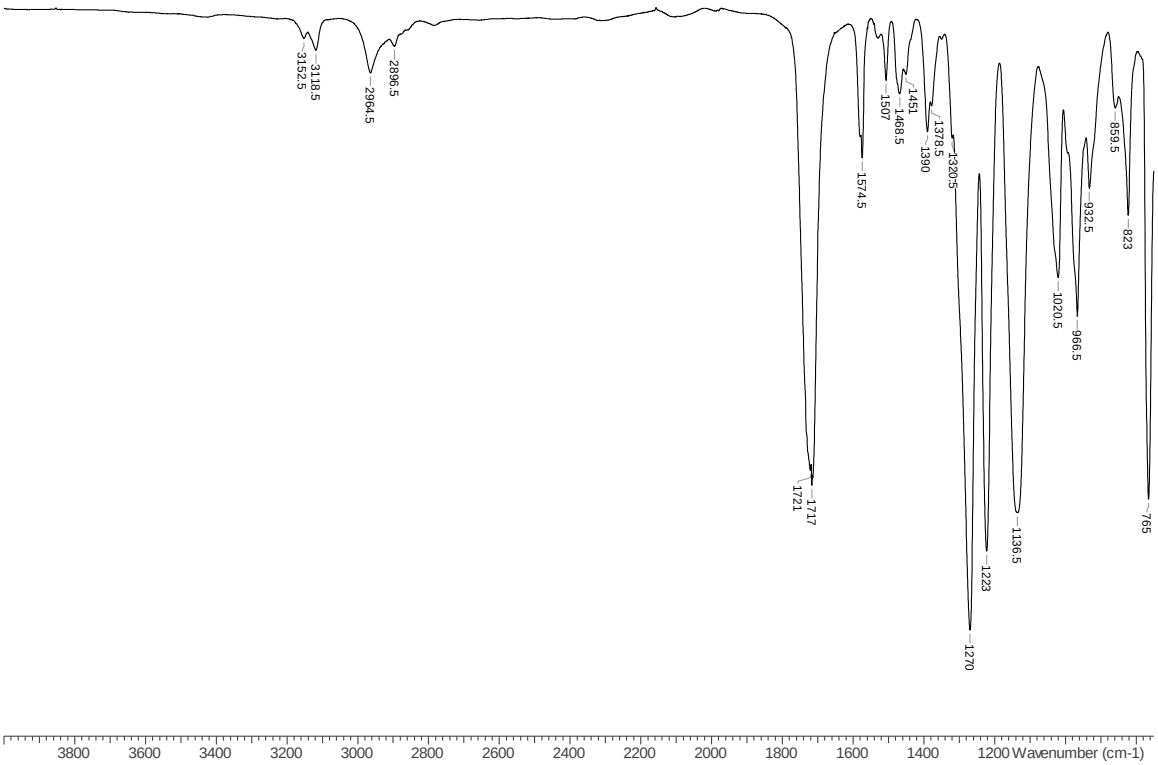

Figure S4a. $PBF_{90}Bf_{10}$ ^{1}H NMR spectrum, CF_3COOD:

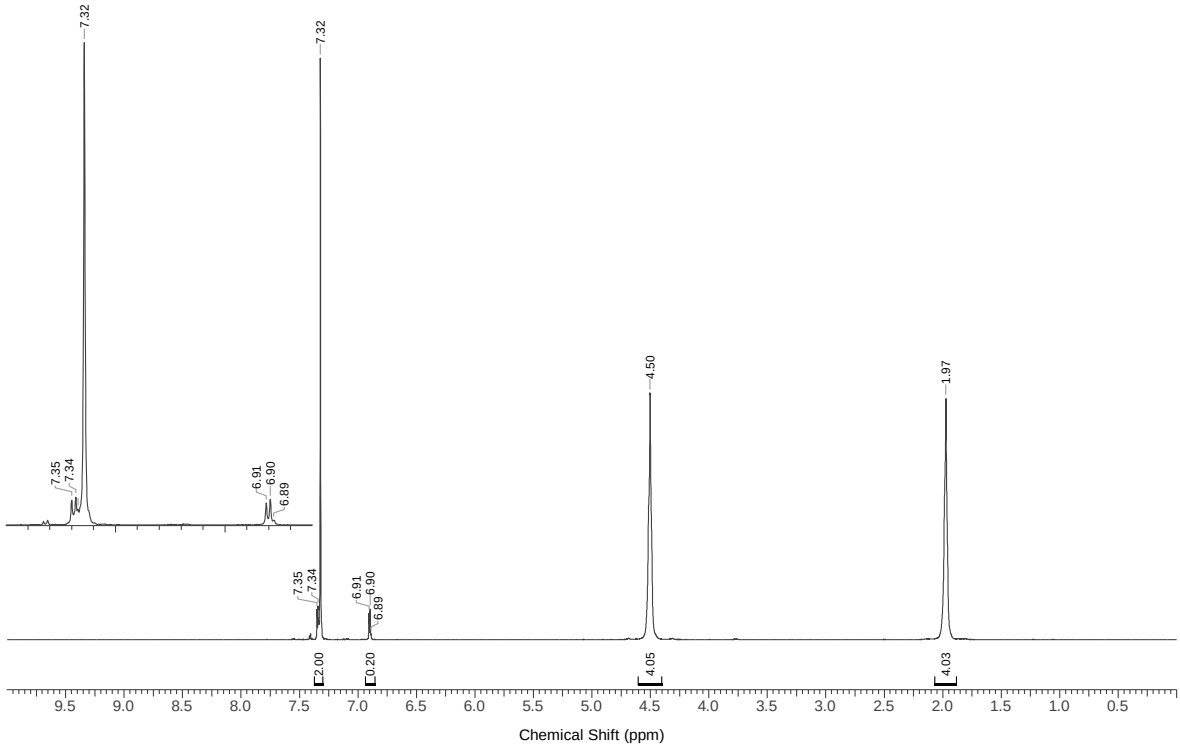

Figure S4b. $PBF_{90}Bf_{10}$ FTIR spectrum:

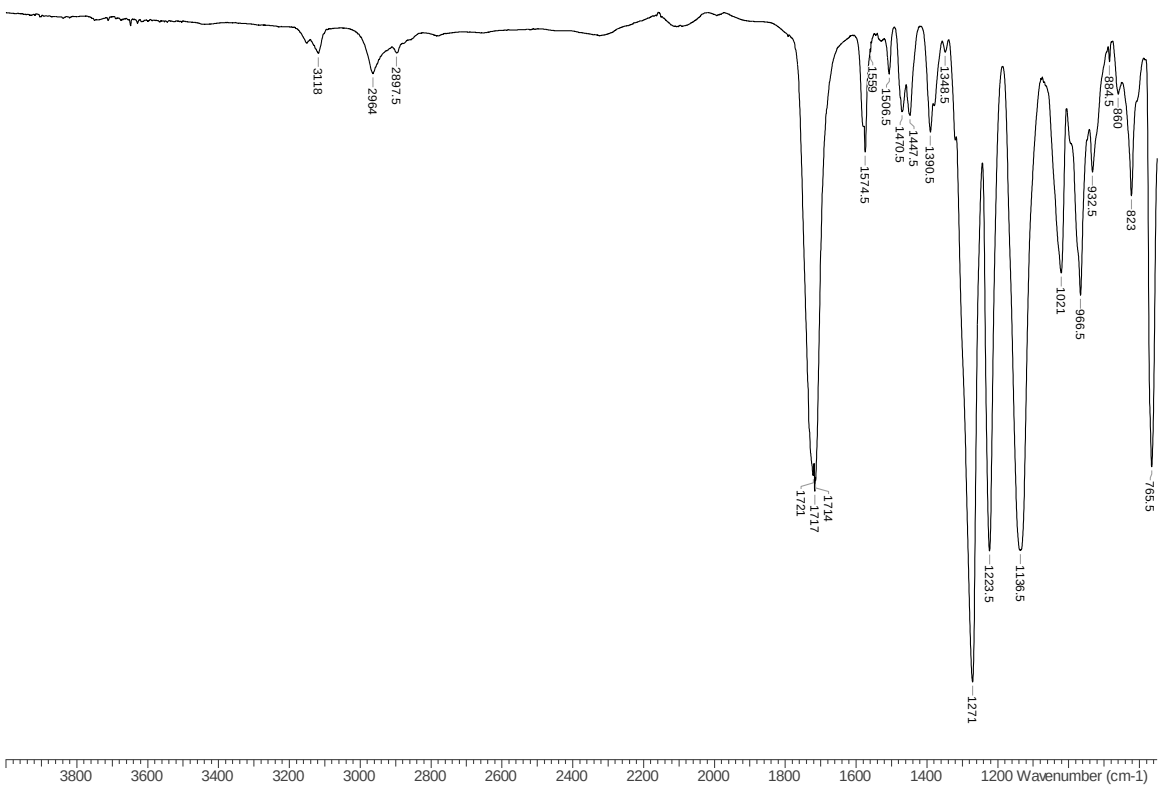

Figure S5a. $PBF_{75}Bf_{25}$ ^{1}H NMR spectrum, CF_3COOD:

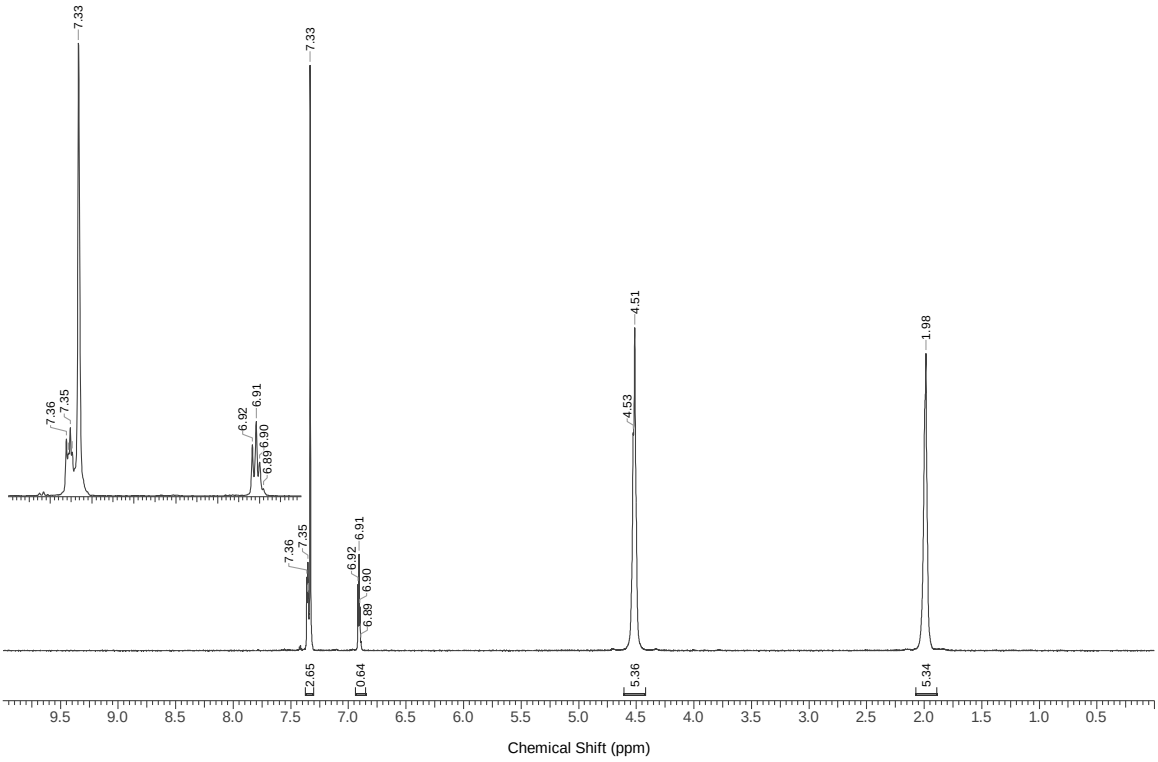

Figure S5b. $PBF_{75}Bf_{25}$ FTIR spectrum:

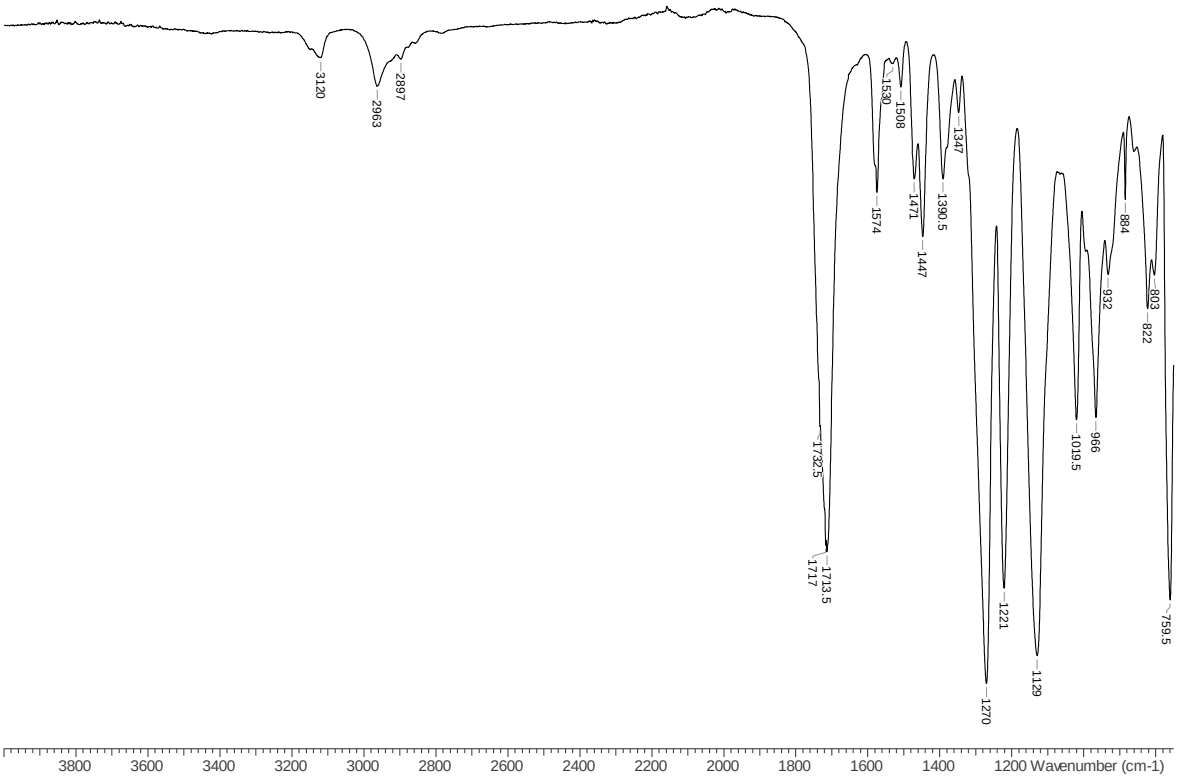

Figure S6a. $PBF_{50}Bf_{50}$ ^{1}H NMR spectrum, CF_3COOD:

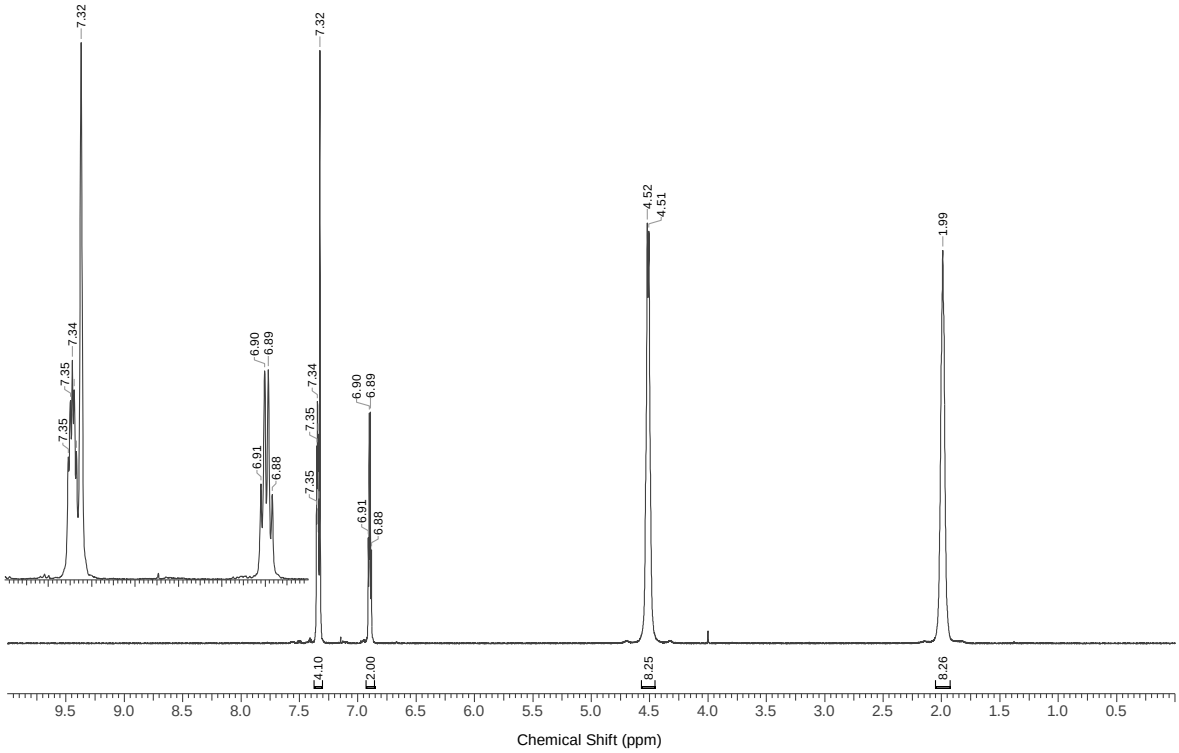

Figure S6b. $PBF_{50}Bf_{50}$ FTIR spectrum:

Figure S7a. $PBF_{25}Bf_{75}$ ^{1}H NMR spectrum, CF_3COOD:

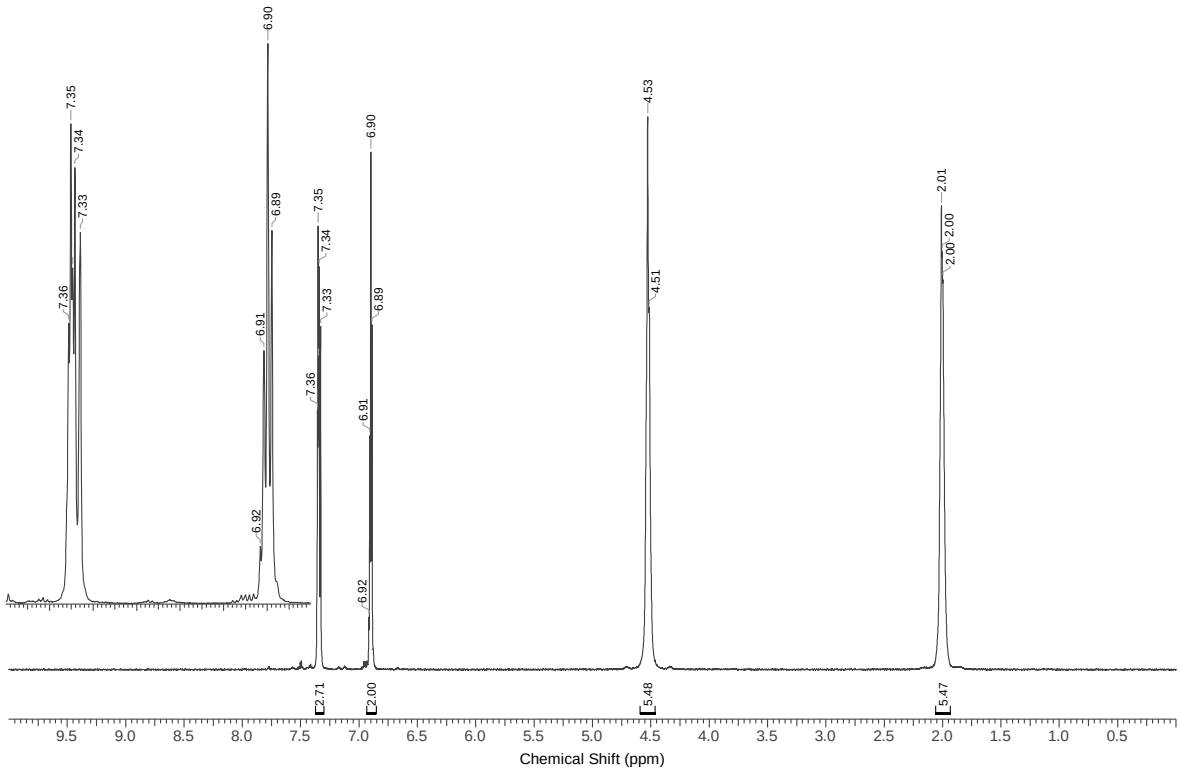

Figure S7b. $PBF_{25}Bf_{75}$ FTIR spectrum:

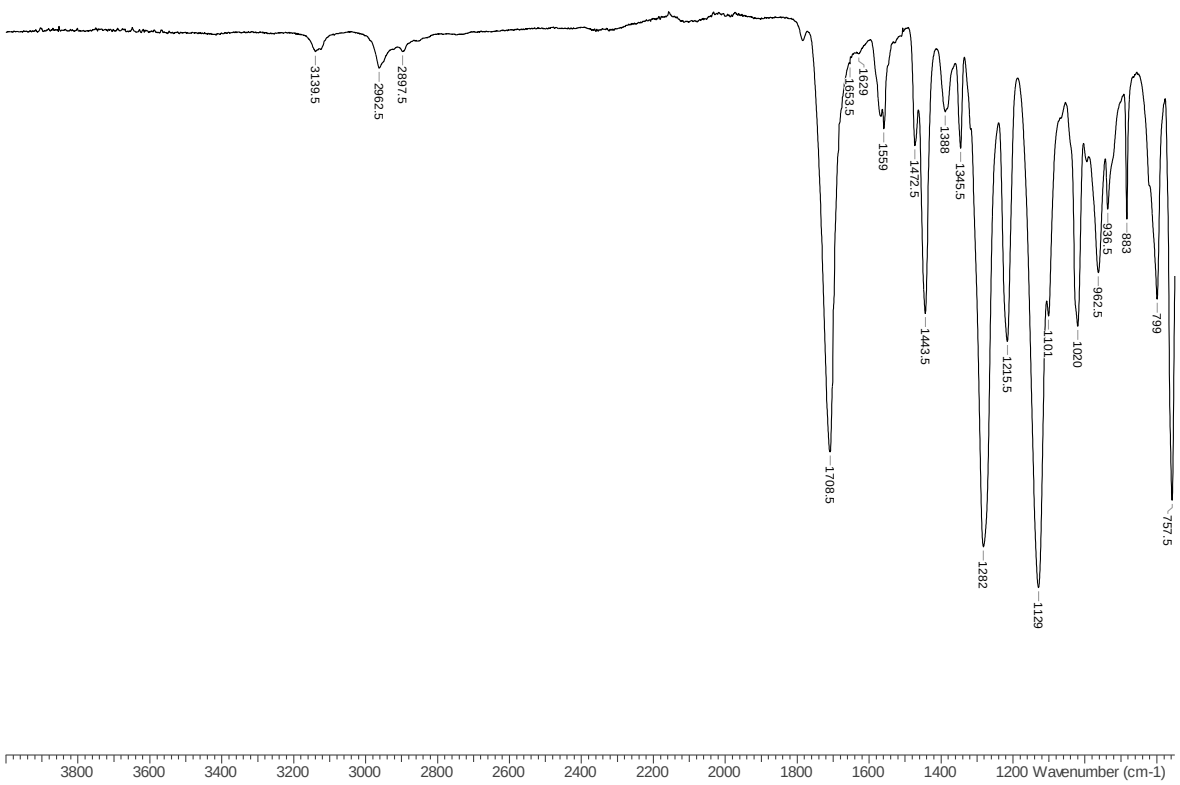

Figure S8a. $PBF_{10}Bf_{90}$ ^{1}H NMR spectrum, CF_3COOD:

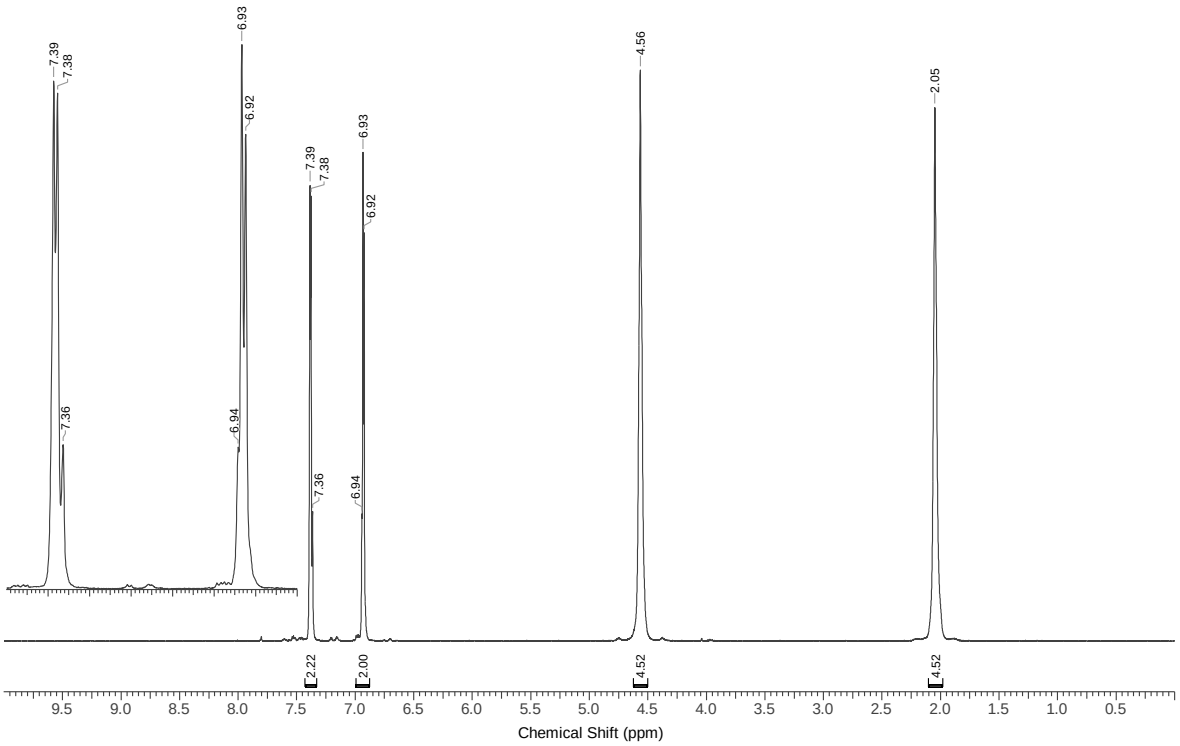

Figure S8b. $PBF_{10}Bf_{90}$ FTIR spectrum:

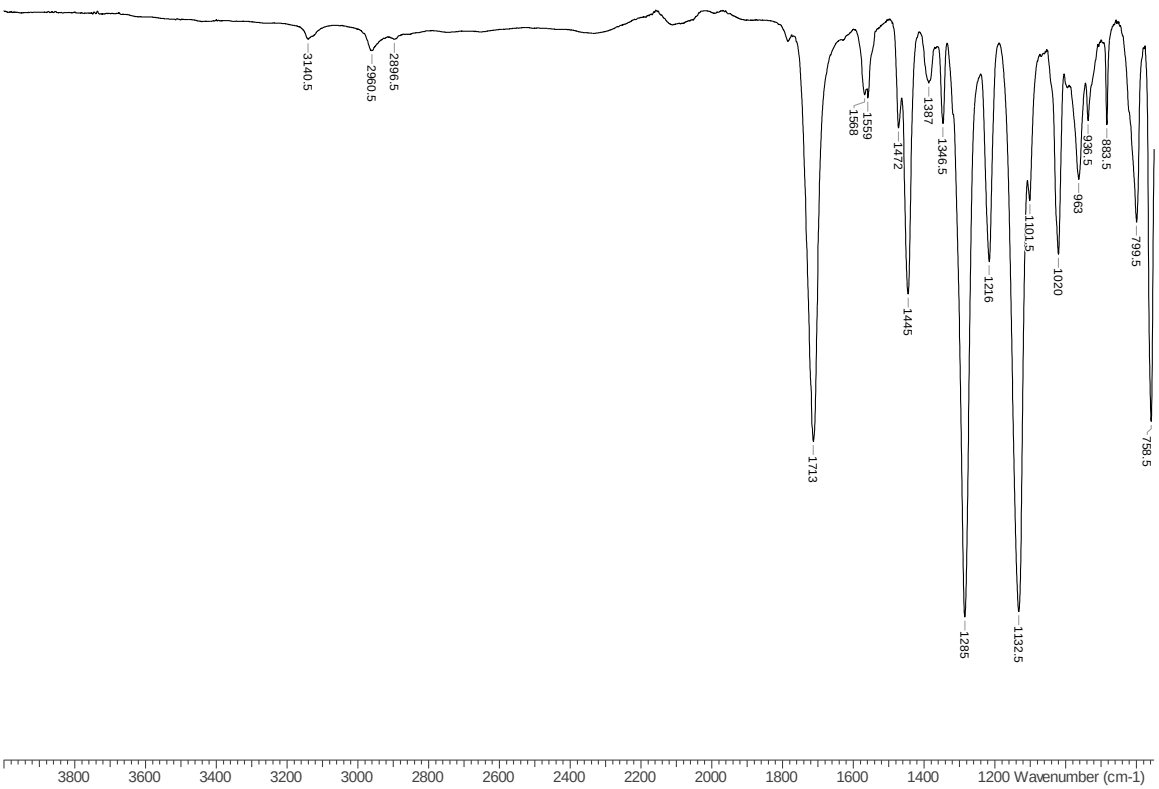

Figure S9a. Poly(butylene bifuranoate) (PBBF) ^{1}H NMR spectrum, CF_3COOD:

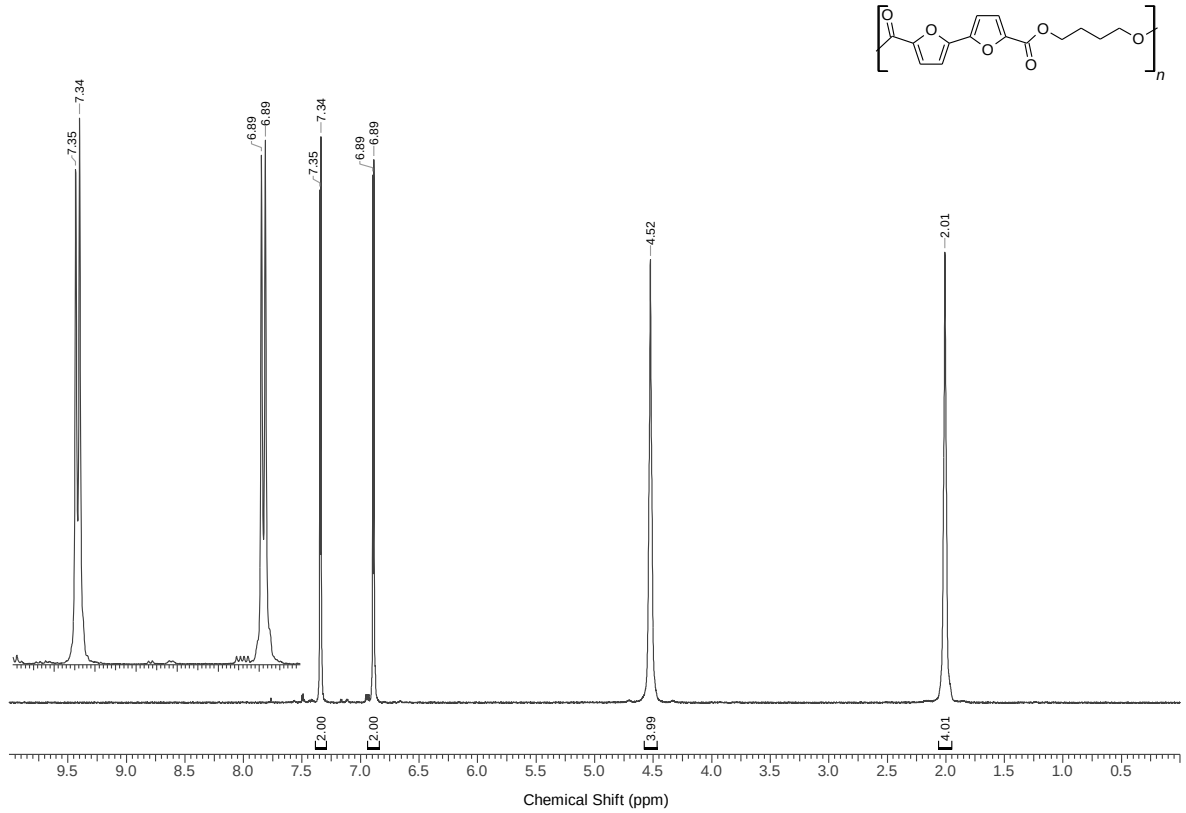

Figure S9b. Poly(butylene bifuranoate) (PBBF) FTIR spectrum:

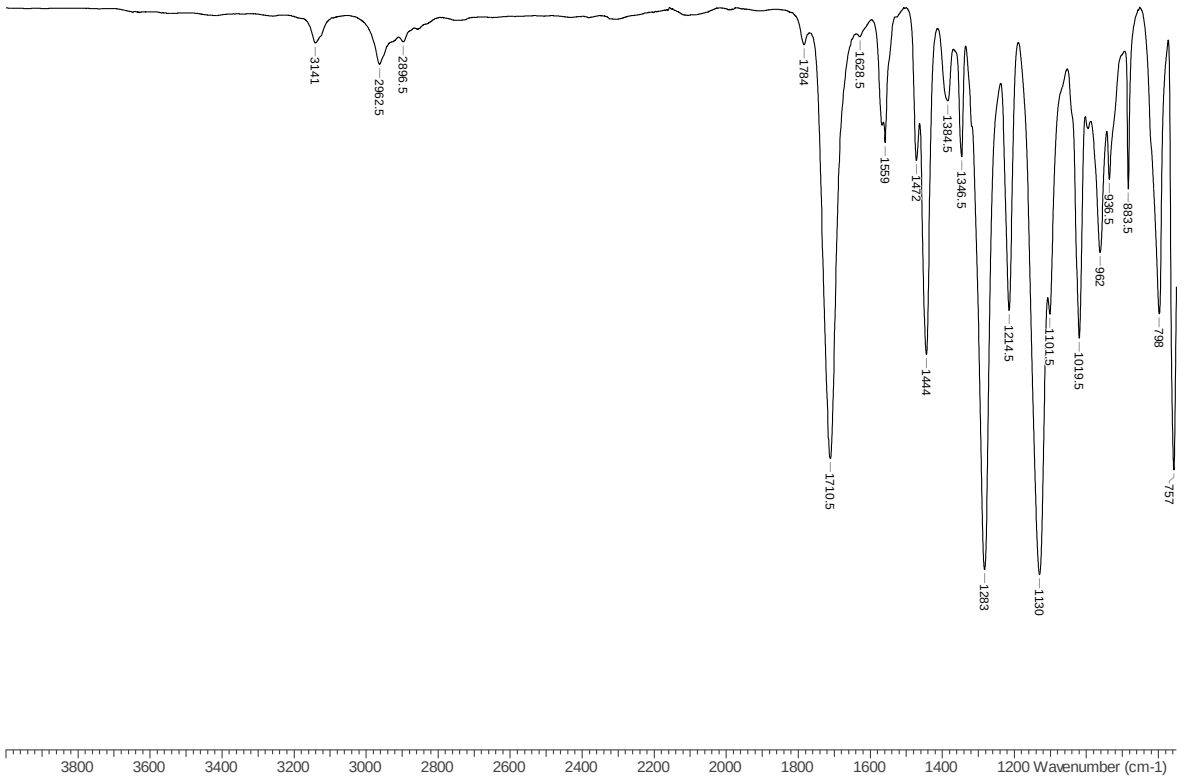

Figure S10. $PBF_{99}Bf_1$ ^1H NMR spectrum, CF_3COOD:

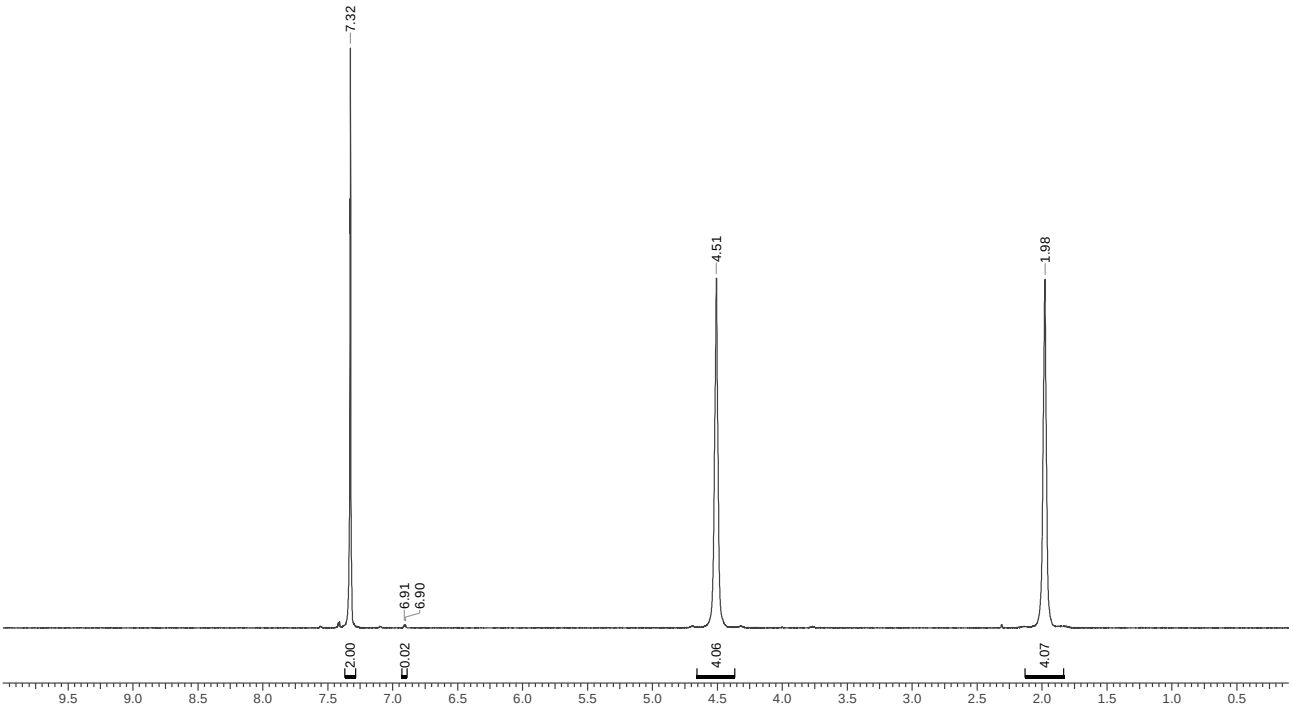

Figure S11. Comparison of FTIR spectra from PBF and PBBf (2800–3300 cm^{-1} and 700–1900 cm^{-1}):

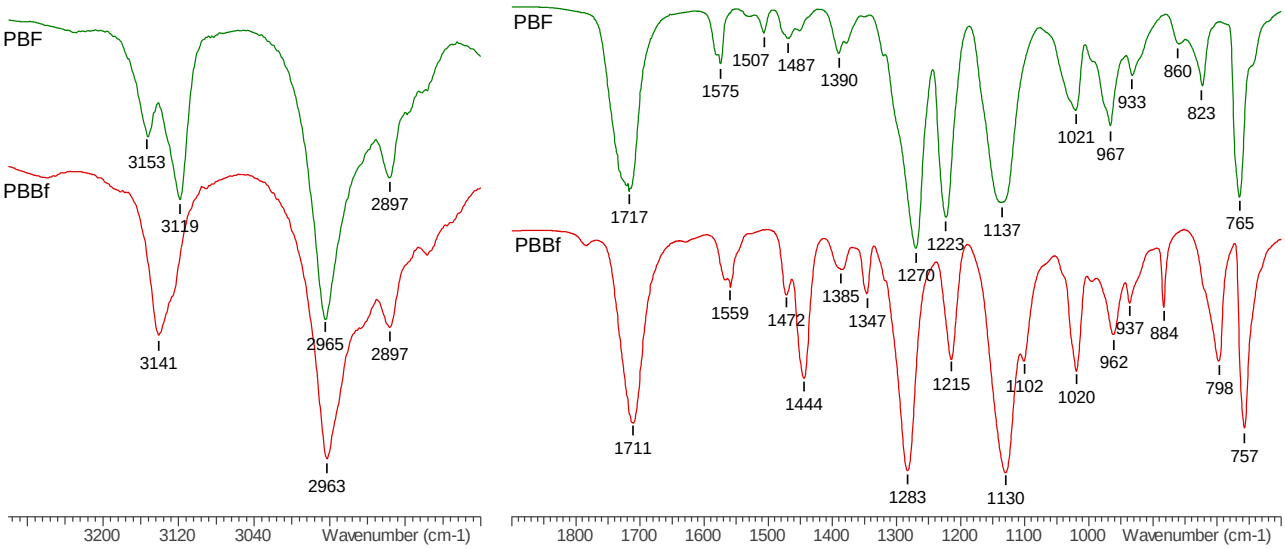

Table S1. Experimental and theoretical IR data for PBF and PBBf

Wavenumber (cm^{-1})					
PBF			PBBf		
Experimental	Theoretical	Assign.	Experimental	Theoretical	Assign.
3153	3178	Furan ν_s(C–H)	3141	3175	Bifuran ν_s(C–H)
3119	3167	Furan ν_{as}(C–H)	3118	3163	Bifuran ν_{as}(C–H)
1717	1758	ν(C=O)	1711	1748	ν(C=O)
1575	1564	Furan ν_{as}(C=C) + δ_{as}(C–O–C)	1559	1550	Bifuran ν_{as}(C=C) + $\delta_{as,ip}$(C–O–C)
-	-	-	1444	1439	Bifuran ν_s(C=C) + $\delta_{s,ip}$(C–O–C)
860	872	Furan τ(H–CC–H)	884	867	δ_{ip}(C–C=C)
823	804	ω(H–CC–H)	798	792	ω(H–CC–H)

Computational Methods

The constitutional repeating units (CRU) of PBF and PBBf were modelled with the molecules shown in Figure S13. The FTIR (500–4000 cm^{-1}) spectra based on the optimized geometries of the PBF and PBBf models were calculated using density functional theory (DFT) with an EDF2 functional and the 6-31G(d) basis set within Spartan '18 Parallel Suite Program, Version 1.3.0, Feb 28 2019. The calculated FTIR frequencies were used to identify some of the experimental vibrational modes. The EDF2/6-31G(d) has been formulated to reproduce the measured infrared frequencies of molecules.[1] We note that here we modelled our polymers with the short CRU structures, which give reasonable wavenumbers and simulation of the vibrational modes to assist in assigning of the experimental frequencies. The calculated frequencies have been corrected for the zero-point vibrational energy with a factor of 0.9620.[1] The absence of the imaginary frequencies ensured that the minimum energy conformations were reached during the optimizations.

[1] https://www.wavefun.com/

Figure S12. Molecular models of the CRUs of PBF (a) and PBBf (b) used in quantum chemical calculations:

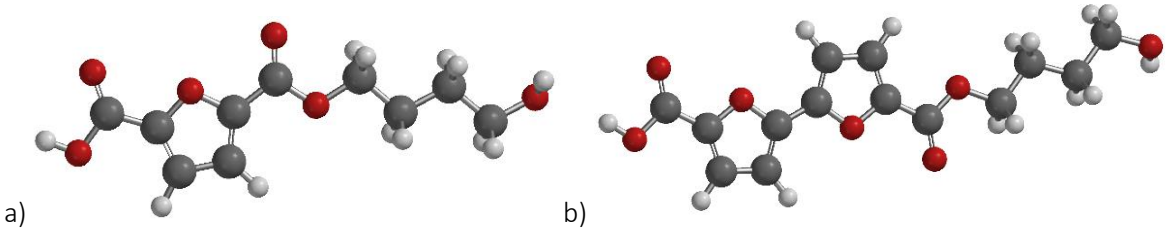

Table S2. Melting enthalpies obtained via DSC

Sample	ΔH_m (J g^{-1}), 1st heating (10 °C/min)*	ΔH_m (J g^{-1}), 2nd heating (10 °C/min)**	ΔH_m (J g^{-1}), 1st heating (5 °C/min)*	ΔH_m (J g^{-1}), 2nd heating (5 °C/min)**
PBF	41.4	35.4	-	-
$PBF_{90}Bf_{10}$	35.6	1.9	35.8	19.6
$PBF_{75}Bf_{25}$	17.9	-nd	19.3	-nd
$PBF_{50}Bf_{50}$	-nd	-nd	-nd	-nd
$PBF_{25}Bf_{75}$	14.5	-nd	27.2	-nd
$PBF_{10}Bf_{90}$	15.7	11.5	35.6	26.9
PBBf	42.2	38.7	-	-

*As received sample, dried at 60 °C for several days under vacuum after solvent precipitation.
**Cooled at the same rate after 1st heating.
nd: not detected

Figure S13. DMA results for polyesters:

a)

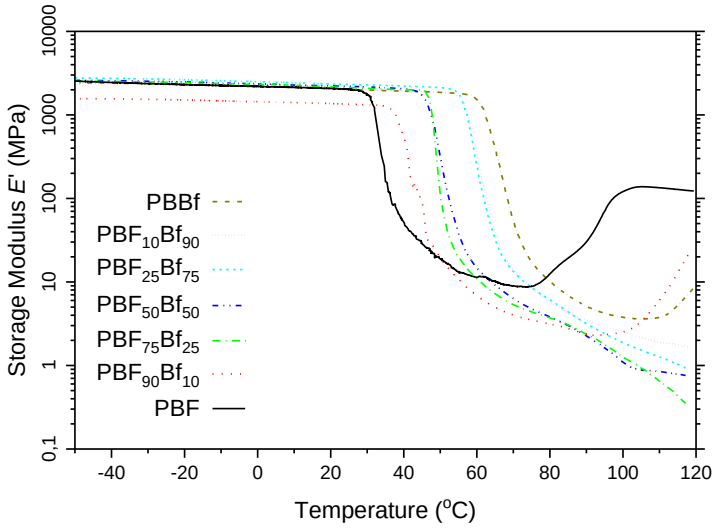

b)

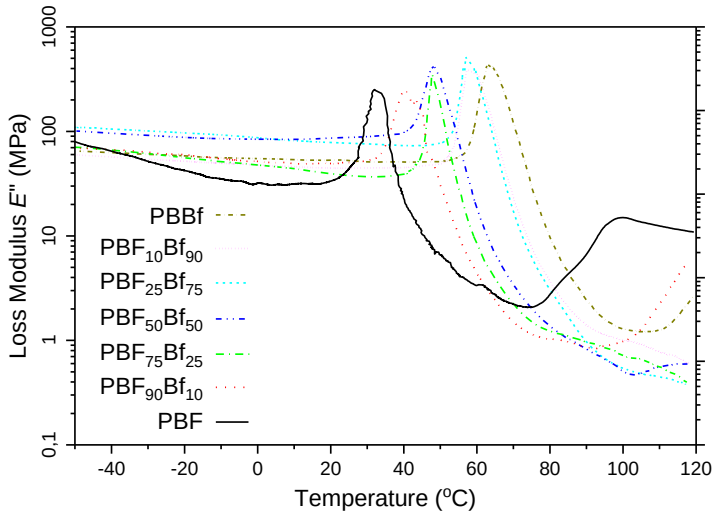

c)

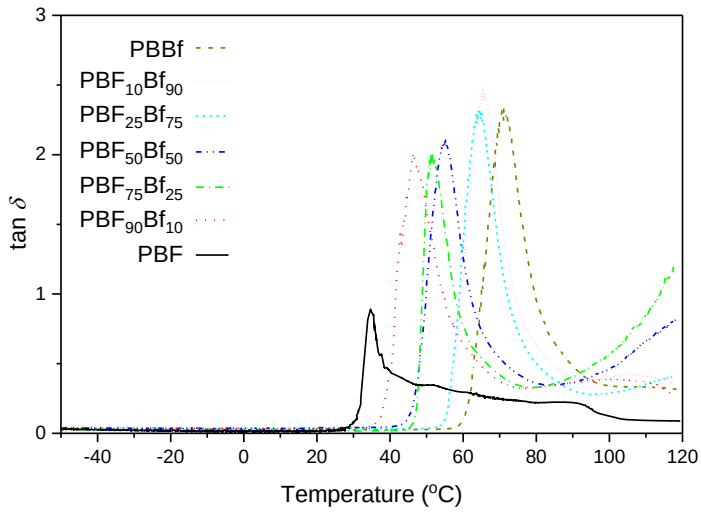

Figure S14. Digital images of melt-pressed PBF and PBBf films obtained by polarized optical microscopy (side-length = 100 μm). The inserts are diffraction patterns of the optical images using the Bertrand lens:

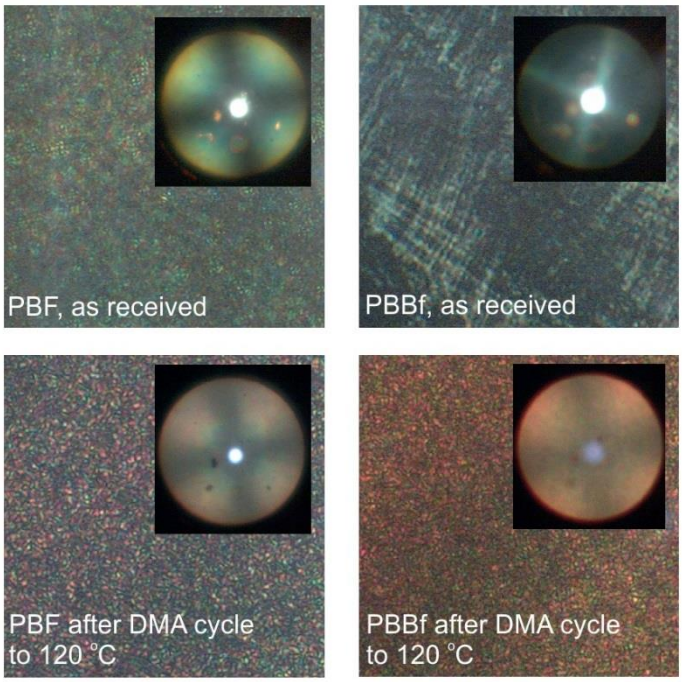

Figure S15. UV-vis absorption spectra of dimethyl 2,5-furandicarboxylate and dimethyl 2,2'-bifuran-5,5'-dicarboxylate in $CHCl_3$ (250–800 nm, 1.0 mg in 100 mL):

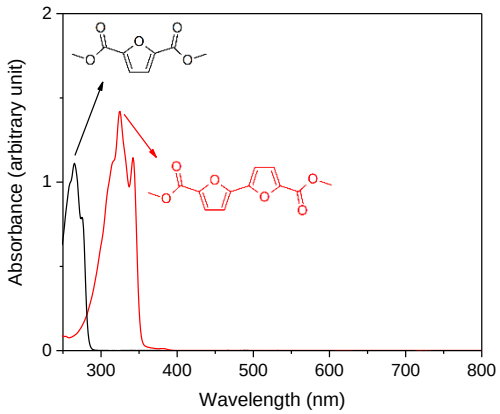

Figure S16. XRD-diffractograms obtained from melt-pressed films: